# Simulations of Wave Impact and Two-Phase Flow with ComFLOW: Past and Recent Developments

*Roel Luppes*
*Henri J.L. van der Heiden*
*Peter van der Plas*
*Arthur E.P. Veldman*
Johann Bernoulli Institute for Mathematics and Computer Science
University of Groningen.
Groningen, The Netherlands

*Bülent Düz*
Department Maritime & Transport Technology
Delft University of Technology.
Delft, The Netherlands

## ABSTRACT

The CFD simulation tool ComFLOW is developed for simulations of two-phase flow and wave impact in offshore and coastal applications. ComFLOW solves the Navier-Stokes equations in both water and air, with second order accuracy. The water surface is advected by means of an improved VOF method, through a local height function approach. Numerical reflections and spurious velocities are prevented by absorbing boundary conditions and gravity-consistent density averaging. The present focus lies on accurate wave propagation, the effect of viscosity in shear layers, regularisation models for turbulence, coupling algorithms for interactive body motion and enhanced numerical efficiency through local-grid-refinement and parallelisation.

KEY WORDS: ComFLOW; VOF; absorbing BC; turbulence regularization; local grid refinement.

## INTRODUCTION

Extreme wave impact can be a serious threat to the land behind coastal protection structures and/or the safety on offshore structures, see Fig. 1. Internal sloshing in a vessel (e.g. a LNG tanker) may also lead to serious problems, in the worst case even to capsize. The CFD simulation tool ComFLOW is developed for the simulation of sloshing liquids (two-phase flow) and wave impact in e.g. offshore applications, to support the design of structures with enhanced reliability, see e.g. Luppes et al. 2011, Veldman et al. 2011.

ComFLOW solves the Navier-Stokes equations in both water and air, with $2^{nd}$-order accuracy in both space and time, through $2^{nd}$-order upwind discretisation in combination with Adams-Bashforth time-stepping. Compressibility of the air can be included, which is especially important in cases of violent flow conditions, when air entrapment occurs. The water surface is advected by means of a modified Volume-of-Fluid (VOF) method, with improved accuracy through a local-height-function (LHF) approach. Numerical reflections are prevented by specially designed absorbing boundary conditions (ABC). Gravity-consistent density averaging for two-phase flow prevents spurious velocities near the free surface. The employed numerical methods make ComFLOW suitable for accurate predictions of wave impact forces.

To further enhance the accuracy of simulations, several aspects in the numerical model in ComFLOW need further extension and improvement. Therefore, a joint industry project (JIP) has been set up, in cooperation with several companies (oil companies, ship yards, classification institutions, engineering companies, etc.). In the ComFLOW3 JIP, the focus lies on accurate wave propagation and the effect of viscosity in shear layers (model small-scale flow details). The numerical efficiency is improved by speed-up through local-grid-refinement techniques and parallelization. Other scientific items that receive attention are multi-dimensional non-reflecting boundary conditions and accurate turbulence modelling on coarse grids with regularization models. Also coupling algorithms for interactive body motion (e.g. wave-vessel interaction) are subject of study.

Fig. 1: Extreme wave impact may result in serious damage and security risks in both coastal and offshore applications.

In this paper, several numerical techniques are described that have been employed successfully in ComFLOW over the years. Several results of the ComFLOW3 project are discussed, together with future plans.

## NUMERICAL METHODS

### Cell Labeling Method

During a simulation, at every time step, grid cells are given labels to distinguish between fluid, air and boundary. Geometry labelling divides the cells into 3 types: flow cells (cells fully or partially open for fluid), **B**oundary cells (fully closed) and e**X**ternal cells (out of consideration).

Free-surface labelling provides a subdivision of flow cells: **E**mpty cells (only air), **S**urface cells (adjacent to an E-cell) and **F**luid cells (remaining flow cells). In one-phase simulations, E-cells are truly empty and are left out of the computations, with free surface boundary conditions prescribed around S-cells. In two-phase simulations, E-cells contain air and are included in the simulation. In Fig. 2, an example of a cell-label configuration is shown.

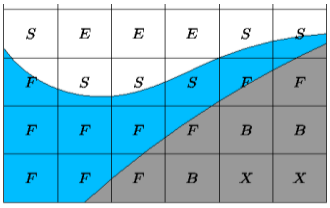


Fig. 2: Example (2D) of cell labeling: dark shading represents solid, blue and white represent water and air, respectively.

## Solving the Navier-Stokes Equations

***Discretisation*.** The equations are coupled through an explicit time-stepping procedure. When time discretisation (time levels n, time step $\Delta t$) is applied to the Navier-Stokes equations for two-phase flow, several terms arise that require further attention: the density $\rho$ and pressure p at the new time level ($\rho_{n+1}$, $p_{n+1}$) as well as the convection term $\nabla.(\rho_n \mathbf{u}_n \mathbf{u}_n)$, with $\mathbf{u}_n$ the velocity at the old time level, see e.g. Luppes et al. 2008, 2010b, Wemmenhove 2008b, Wemmenhove et al. 2006, 2007, 2008a, 2009, 2012.

Spatial discretisation is done on a staggered Cartesian grid, with the pressure located in cell centers and velocities in the middle of cell faces. The convection term, which dominates in case of momentum-driven applications, is treated with symmetry-preserving upwind spatial discretisation (Verstappen and Veldman, 2003). With 1st-order upwind (B2), artificial diffusion is applied to obtain stable solutions, possibly leading to an abundant damping of fluid motion. Using the 2nd-order upwind (B3) scheme, the level of artificial diffusion is much smaller, usually resulting in an acceptable level of damping. B2 can be combined easily with 1st-order Forward Euler (FE) time discretisation, but for B3 an alternative time discretisation is needed to obtain stable solutions. In ComFLOW, the explicit 2nd-order Adams-Bashforth (AB) method is used, as it is relatively easy to implement. Methods that use intermediate time levels (e.g. Runge-Kutta methods) cannot be used, since the liquid configuration is not properly known between two time levels. The combination of B3 spatial- with AB time-discretisation makes ComFLOW 2nd-order accurate in both space and time.

Both combinations FE+B2 and AB+B3 are limited in their stability by the CFL number $\eta = u\,\Delta t/\Delta x$ and diffusion number $d = 2\mu\,\Delta t/\Delta x^2$. In most practical offshore and coastal cases, convection dominates diffusion, and the CFL number predominantly controls the stability limit. For the combination B2+FE, the CFL limit is $\eta < 1\text{-}d \approx 1$. For B3+AB this limit is more restrictive: $\eta < ¼ - ½d \approx ¼$. This means that B3+AB requires a 4 times smaller $\Delta t$; the price to reduce artificial damping of fluid motion (Luppes et al. 2008, 2009b, 2010b, Wemmenhove 2008b).

***Poisson equation*.** The pressure $p_{n+1}$ is calculated from a Poisson equation, which follows from combination of the momentum and continuity equation. Initially, this equation contains $\delta\rho/\delta t$ and $\nabla\rho$, and hence experiences large variations, because of the large $\rho$-ratio (water vs. air). Therefore, the term $\rho_{n+1}$ in the equation is substituted analytically by the gas density $\rho_g$, which gives

$$\Delta t\,\nabla.(\nabla p_{n+1}/\rho_n) = \chi\,[\,(\rho_{g,n+1} - \rho_{g,n})/\Delta t + \mathbf{u}_n \nabla\rho_{g,n}\,]/\rho_n + \nabla.\mathbf{v}, \qquad (1)$$

with $\chi = (F_B\text{-}F_S)/F_B$, where $F_B$ denotes the fraction of a computational cell open for fluid (so-called apertures) and $F_S$ the fraction of that cell filled with liquid. The term **v** (dimension m/s) includes convection, diffusion and external forces (gravity). In Eq. 1, the spatial derivatives of $\rho$ no longer contain large variations, as they are only determined by compression and/or expansion of the gas phase. The term $\rho_{g,n+1}$ is subsequently reformulated in the gas pressure $p_g$ through an equation of state. The treatment of this term, in combination with $\nabla\rho_{g,n}$, is e.g. described in Luppes et al. 2008, 2010b, Wemmenhove 2008b. Finally, $p_g$ is linearised by a Newton approximation and then transferred to the left-hand side of the Poisson equation.

In case of two-phase flow, the entries in the Poisson matrix ***M*** may differ up to a factor 1000, because of the jumps in $\rho_n$ (water vs. air). Hence, a powerful matrix solver is needed. In ComFLOW, the Poisson equation $\boldsymbol{M}p_{n+1} = \text{RHS}$ is solved with contemporary sparse-matrix techniques, viz. a Krylov subspace method with incomplete LU preconditioning for acceleration. For one-phase flow simulations, the pressure is solved with SOR, where the optimal relaxation parameter is adjusted automatically during the iterations; based on Botta and Ellenbroek 1985, but further improved to enhance computational efficiency. For both methods, iteration is continued until the maximum relative residual $r = (\boldsymbol{M}p_{n+1} - \text{RHS})/p_{n+1} < 10^{-8}$. In that case, the obtained pressure and (divergence-free) velocity field are sufficiently accurate, which also ensures accurate mass conservation. The required number of iterations usually depends on the number of grid points, the grid stretching, the apertures $F_B$ and the fluid configuration $F_S$, as these are all 'felt' by the Poisson matrix ***M***. Obviously, the $F_S$ distribution strongly depends on the nature of the simulated problem (violent sloshing versus 'smooth' waves).

## Accurate Free-Surface Displacement

ComFLOW has been developed initially to study sloshing fuel on board spacecraft in micro-gravity, for which a very accurate and robust description of the free surface is required (Veldman et al. 2007, Veldman 2006, Luppes et al. 2005, 2006, 2009b). Later, the methodology was extended to simulations of sloshing liquids and two-phase flow in offshore and coastal applications. The Cartesian grid in ComFLOW provides a simple geometrical framework in which the position and slope of the free surface can be accurately described. On unstructured grids the reconstruction of the free-surface would be more difficult. There, reconstruction often results in smearing of the free surface, which erroneously reduces peak pressures and hence leads to less accurate wave-force predictions on unstructured grids.

In ComFLOW, an improved volume-of-fluid (VOF) method (originally by Hirt and Nichols 1981) is applied to describe the evolution of the free surface. In principle, the motion of the free surface is described by an advection equation for $F_S$. However, numerically the free surface displacement is done in a different way. First it is reconstructed and then it is advected to the new position. In the employed VOF method, filling rates $F_S$ of individual cells are administrated and fluid fragments are advected with local velocities. The free surface position is subsequently reconstructed from combined fluid volumes contained in single cells. Traditionally, the reconstruction is done with Simple Linear Interface Calculation (SLIC), where the interface consists of line segments that are constructed either parallel or perpendicular to the major flow axes. A characteristic drawback of SLIC is the unphysical

creation of disconnected droplets, resulting from errors in the reconstruction. Moreover, in the original VOF method values have to be rounded off ($0 \leq F_S \leq 1$) at the end of the displacement algorithm at each time step, leading to significant losses in liquid mass.

To prevent from isolated droplets and mass losses, a local height function (LHF) has been introduced in ComFLOW (Veldman et al. 2007, Veldman 2006, Kleefsman et al. 2004, 2005a, 2005b, Luppes et al. 2005, 2006, 2009b, 2010a, 2010b, 2011). The LHF is applied in a block of cells surrounding a central S-cell. First, the orientation of the free surface is determined (in 2D either horizontal or vertical), depending on the filling rates $F_S$ in the surrounding block of cells. Next, the horizontal or vertical height in each row or column is computed by summing $F_S$ values, see Fig. 3. Based on the LHF, fluid is transported from one cell (donor) to another (acceptor), depending on the magnitude of local velocity, time step and grid sizes. In this way, the interface is explicitly reconstructed through a LHF and subsequently advected. The free-surface at the new time instant is then reconstructed by means of another LHF. The employed technique ensures a sharp interface without smearing, which is essential for accurate simulations of wave impact forces.

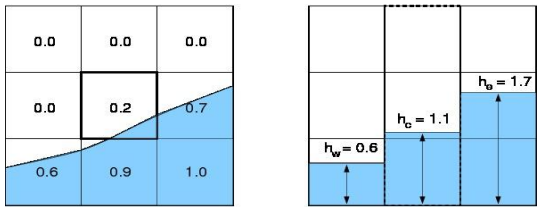


Fig. 3: Construction of the LHF around a central S-cell by summing $F_S$ values vertically.

In Fig. 4, the liquid configurations after two simulations of a breaking dam, with and without using LHF, are depicted. The LHF approach in ComFLOW clearly results in significantly less erroneous droplets compared to the original VOF method and is strictly mass conserving. These are the two major improvements of the unfavorable numerical artifacts of the original VOF method (Veldman et al. 2007, Kleefsman et al. 2005a). The remaining droplets are predominantly located on the tank wall, as in the experiment.

In the ComFLOW3 project, higher-order free-surface reconstruction methods (Youngs, LSG, MYC) and advection methods (MACHO, COSMIC, EI-LE) are subject of study, see Düz et al. 2013. These will probably be used in the future, because of their great potential in accurately simulating wave propagation, especially on coarser meshes. First tests indicate that the combination LSG+MACHO outperforms other combinations and indeed reduces (numerical) wave damping considerably. However, the reconstruction methods (e.g. piecewise linear reconstruction, PLIC) are far more difficult to implement and the computational costs for the reconstruction of the free surface (the plane normal and esp. the plane constant) are strongly enhanced. These disadvantages are certainly significant near cut-cells; near solid obstacles probably the SLIC method with LHF has to be used anyway. Fortunately, for many wave-impact and sloshing simulations carried out with ComFLOW, the SLIC method with LHF improvement is sufficiently accurate, particularly on fine grids.

## Gravity-Consistent Density Averaging

In case of two-phase flow, the discrete treatment of the density ρ near the free surface is important. For compressible two-phase flow, ρ in the cell center is given by $\rho = \{F_S \rho_L + (F_B - F_S) \rho_g\} / F_B$, with $\rho_L$ the constant liquid

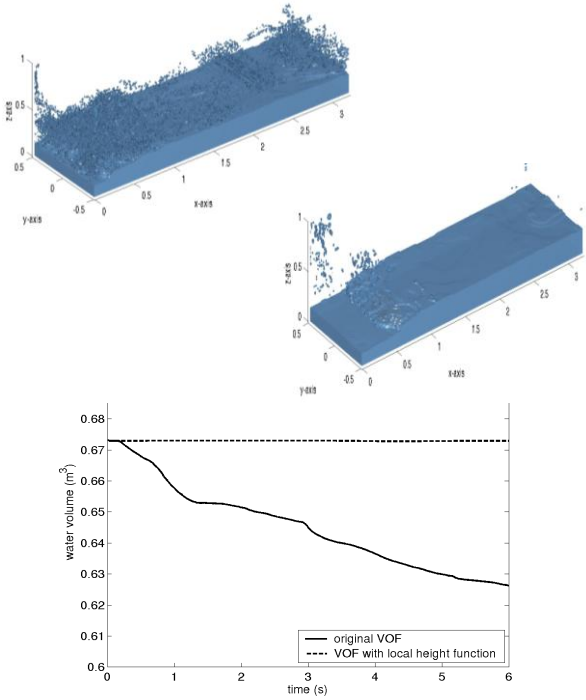


Fig. 4: The use of LHF (middle) results in significantly less erroneous droplets, compared to the original SLIC/VOF method (top), and is perfectly mass-conserving (bottom).

density, and gas density $\rho_g$ a function of p, also located in cell centers. However, ρ is required at velocity locations as well, because of the staggered arrangement of variables (see Fig. 5). The simple geometrical average $\rho_{i+½} = (\rho_i + \rho_{i+1})/2$ may result in spurious velocities, especially in case of high ratios of ρ (water vs. air), and eventually cause severe instabilities near the free surface. These are usually damped with suppression techniques, e.g. by adding diffusion. In ComFLOW, a superior technique is employed, which can be deduced by considering the momentum equation for a fluid at rest (hydrostatic conditions, zero velocities). This reduces to $\nabla p = \rho \mathbf{g}$ and hence to $0 = \nabla \times \nabla(\rho \mathbf{g})$, with **g** the gravity. This condition should also hold for the discrete variables, otherwise velocity terms in the momentum equation no longer vanish and consequently spurious velocities are generated. This leads to a requirement how ρ should be averaged. Formulas that satisfy this requirement are called `gravity consistent'. A gravity consistent average is found by looking at the momentum control volume (the red-dashed region in Fig. 5) and weight the neighboring density values with the fraction that this control volume is split by the free surface (Wemmenhove et al. 2007, 2008a, 2009, 2012, Wemmenhove 2008b, Veldman et al. 2011).

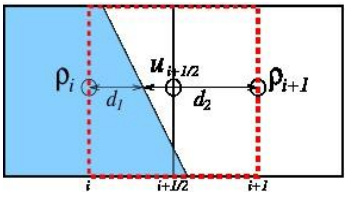


Fig. 5: The gravity-consistent density average $\rho_{i+½}$ is found by weighting $\rho_i$ and $\rho_{i+1}$ with the fraction (coefficients $d_1$ and $d_2$) that the free surface splits the red-dashed momentum control volume.

The difference between simple and sophisticated density averaging for a simple hydrostatic case is shown in Fig. 6 (top row). Simple geometrical averaging leads to spurious velocities (left). With gravity consistent averaging, the oblique free surface stays at rest, perpendicular to the gravity (right). The effect on the free surface for a regular sway sloshing experiment (with 10% filling ratio) is shown in Fig. 6 (bottom row). Naive geometrical averaging clearly results in instabilities (left), whereas gravity consistent averaging results in much less disturbances near the free surface (right).

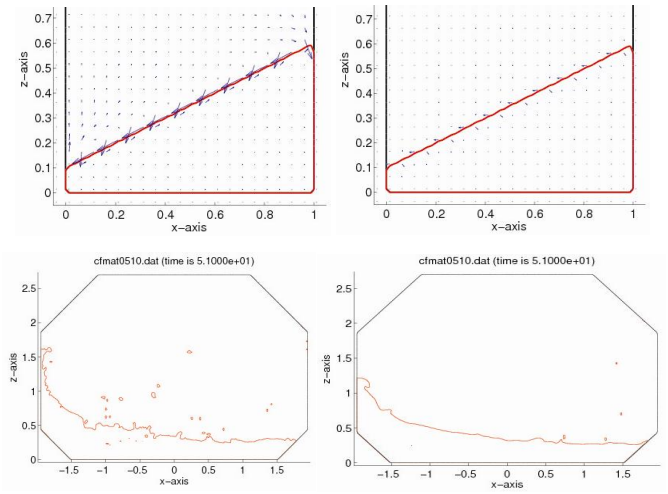


Fig. 6: Top row: hydrostatic case, with gravity **g** = (1,-2) perpendicular to the oblique free surface. Bottom row: liquid configuration after two simulations of a regular sway sloshing experiment. With sophisticated gravity-consistent density averaging (right) much less instabilities are observed than with simple geometrical averaging (left).

## ABSORING BOUNDARY CONDITIONS (ABC)

For simulations with open boundaries, an ABC has been designed for ComFLOW that suppresses numerical wave reflections from the boundaries. Consequently, open boundaries can be located relatively close to a structure, without influencing outgoing waves or generating numerical reflections that affect water waves inside the flow domain. At the same time, regular or irregular waves can enter the flow domain as prescribed. In this way, less grid-points are required compared to traditional damping-zone techniques, and hence computing times are reduced considerably (Luppes et al. 2009a, 2010a, Wellens et al. 2009).

### ABC for 2D Waves

The ABC is an extension of the Sommerfeld condition for a potential $\Phi$, i.e. $(\delta/\delta t + C_{out}\,\delta/\delta x)\,\Phi_{out} = 0$. Sommerfeld is fully absorbing for one single outgoing wave component (phase velocity $C_{out}$), but gives reflections for waves composed of components with other phase velocities C(k) arriving at the boundary (k denotes the dimensionless wave number Kh). The constant function $C(k) = C_{out}$ is actually a poor (constant) approximation of the dispersion relation. The dispersion relation can also be approximated by a rational function: $C(k) \approx \sqrt{(gh)}\,(a_0+a_1k^2)/(1+b_1k^2)$, with higher accuracy for a wider k-range when the coefficients $a_0,a_1,b_1$ are optimally tuned. As a result, the reflection (-coefficient) of the ABC is an order of magnitude smaller for that range. Since $\Phi$ satisfies $k^2\,\Phi_{out} = \delta^2\Phi_{out}/\delta z^2$, k can be replaced by 2nd-order derivatives along the boundary, which leads to

$$[\,(1+ b_1h^2\,\delta^2/\delta z^2)\,\delta/\delta t + \sqrt{(gh)}\,(a_0+ a_1\,h^2\,\delta^2/\delta z^2)\,\delta/\delta x\,]\,\Phi_{out} = 0. \qquad (2)$$

The numerical implementation of the ABC (Eq. 2) at an outflow boundary, which coincides with the location of the horizontal velocity u, is described in Wellens et al. 2009. In short, first the derivatives of $\Phi$ in Eq. 2 are formally replaced through $\delta\Phi/\delta x = u$ and the Bernoulli equation $\delta\Phi/\delta t = -p-gz$. The momentum equation is then used to eliminate the velocity $u_{n+1}$, which stems from discretisation of $\delta u/\delta t$. The final result is a boundary condition for the pressure p. It can easily be combined with the internal pressure Poisson equation, but has a larger stencil, which makes it more difficult to solve. A powerful Krylov method is needed, with incomplete LU-preconditioning for acceleration; the price to reduce spurious reflections.


Fig. 7: The two domains used to test the performance of the ABC. A short domain, with either Sommerfeld or ABC imposed at $x_{out}$, and the long domain with boundary at $x_{end}$. Reflections at $x_m$ are measured from the difference between long and short domains.

The performance of the ABC can be investigated (Wellens et al. 2009, Luppes et al. 2009a, 2010a) by comparing the free surface at a measurement position ($x_m$=200m) in two simulations, with either ABC or Sommerfeld at the outflow (located at $x_{out}$=400m), see Fig. 7. As a reference, also a very long domain ($x_{end}$ = 2000m) is considered, where the surface elevations at $x_m$ cannot be disturbed by reflections from the outflow at $x_{end}$. An ensemble of irregular waves (wave height H=4m, peak period T=15s, water depth d=100m) is simulated several wave periods. Any difference at $x_m$ between long and short domain can only be attributed to reflections resulting from the applied boundary condition at $x_{out}$. The performance of the ABC is much better than the Sommerfeld condition and accords well with theory. This is also observed for wave simulations around a semi-submersible, for which both the accuracy and the computational efficiency clearly improve.

The ABC has also been compared to simulations with a traditional pressure-damping zone technique to prevent wave reflections. In this method, an additional free surface pressure is used, proportional to the vertical velocity w at the free surface, which counteracts wave motions. When w≈0 (long waves), pressure damping is not very effective, unless very long dissipation zones are used. This however significantly adds to the computational effort. With ABC both reflections and computing times are considerably smaller.

### Extensions of the ABC

In the ComFLOW3 project, the ABC has been extended for waves entering the domain under an angle α and leaving in other directions. For this, Eq. 2 has been modified by including direction cosines. Differences between numerical results and analytical wave profiles are small, for any α, and for a wide range of wave types. To study wave impact on a structure, ComFLOW users now have two possibilities: keep the position of the structure fixed and vary the incoming angle α, or rotate the structure and keep α constant. Moreover, one can also cut-off the domain at all boundaries, which saves computing time considerably. Again, reflections can be measured from differences between small and large domain, see Fig. 8. For an incoming 5th-order

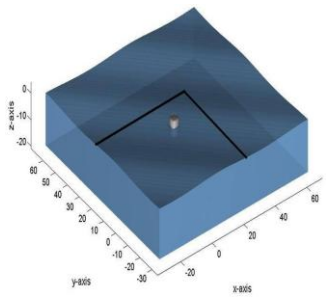

Fig. 8: For waves entering the domain under an angle α, outflow boundaries can be taken close to the structure, at both x- and y-planes, which saves computing time significantly.

Stokes wave with $\alpha=45^{o}$, the observed difference is below 2% up to 3 wave periods of simulation time, see Düz et al. 2011a, 2011b, 2012.

In the future, an even more accurate ABC will be implemented. The ABC will be adapted for non-linear and extreme waves and the effects of stationary currents will be included. For this, the 2nd-order Higdon condition will be considered, i.e. a higher-order Sommerfeld condition. Unfortunately, the Poisson matrix will become even more complex (larger stencil) and probably a dedicated Poisson solver will be employed to maintain computational efficiency.

## REGULARISATION MODELING AND VISCOUS EFFECTS

In many practical coastal and offshore applications the role of viscosity is significant, e.g. when predicting drag forces on the pillars of oil drilling rigs, or the sloshing modes in drilling holes in floating production units. Hence, for an accurate prediction of hydrodynamic forces and resistance due to viscous effects, a careful treatment of viscous wall and free shear flow is required. At least the large-scale viscous flow effects should be described accurately.

### Discretisation of Diffusion

As viscous effects originate from the structure, the discretisation of diffusion near solid walls has been improved. In ComFLOW, a cut-cell immersed boundary approach is used to describe solid geometries, where apertures describe the cell volume or face ratios that are open for flow. The discretisation of shear stresses ($\delta u/\delta y$, $\delta v/\delta x$, etc.) has been refined, making careful use of aperture information. For this, the 2D LSSTAG method (Cheny and Botella 2010) has been adopted (Fig. 9, left) and converted into 3D. In 3D roughly 100 cut-cell cases have been considered, which however can be found largely by rotating a few basic cases (Van der Heiden et al. 2012, Van der Plas et al. 2012). Normal stresses ($\delta u/\delta x$, $\delta v/\delta y$, $\delta w/\delta z$) are discretised in cell centers, analogous to pressure gradients, where the correct formulation in terms of cell face apertures follows upon application of the Gaussian identity.

Already for simple test cases the improvement is clear. For a 2D Hagen-Poiseuille flow, analytical profiles are far more accurately simulated, as shown in Fig. 9 (right). The new method is close to 2nd order (in grid space), whereas the old method is only 1st order.

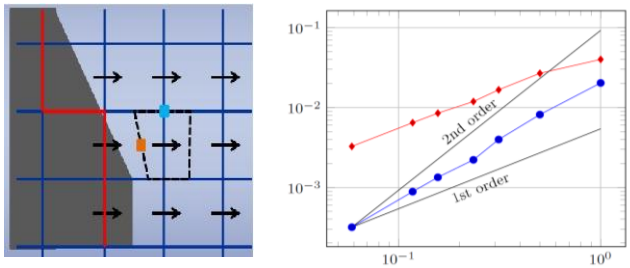


Fig. 9: Left: the LSSTAG discretisation of momentum diffusion is based on the deformed momentum control volume (dashed region), making careful use of aperture information. Right: difference between numerical and analytical velocity ($L_2$-norm) for Hagen-Poiseuille flow; with (red) and without (blue) improved discretisation of diffusion.

#### Regularisation Turbulence Modeling

In many practical coastal and offshore applications, turbulence is responsible for a wide range of scales of motion. The required resolution for the small scales would lead to excessive computing time. Therefore, in ComFLOW an `energy-preserving' turbulence model is implemented, which gives an accurate description of the large-scale flow effects, even on coarse grids. The production of small scales is controlled by a special treatment of the convection term, instead of adding eddy-viscosity (Verstappen 2008, 2011). It is consistent with the energy-preserving discretisation methods that are already employed in ComFLOW. The regularisation approach smoothens the convection term C(u,v) in the Navier-Stokes equations, to restrain the production of small scales. A symmetric self-adjoint filter is used to filter the scales below a certain threshold. This leads to a 2nd-order (in filter length) accurate approximation of the convection term, viz.

$$C_2(u,v) = \overline{C(\overline{u}, \overline{v})}, \qquad (3)$$

where the overline means application of the filter. The great virtue of this model is that it conserves important physical quantities (energy, enstrophy, helicity), like the original convection term. Especially energy conservation is crucial for correct prediction of large scale flow. In laminar parts of the flow, there is no additional dissipation, as $C_2 \approx C$ for low Re numbers. Currently, simple 3-point filters are used, i.e.

$$\overline{u_i} = (L/2\Delta x)\,(u_{i+1} + u_{i-1}) + [1-(L/\Delta x)]\,u_i, \qquad (4)$$

where $0 \le L \le \Delta x$ resembles the filter length. The magnitude of L is determined from the requirement that the convective production of sub-grid scales is counteracted by diffusive dissipation of the same scales.

As a test case, the vortex shedding behind a circular cylinder is studied (Re=2000), with different treatments of convection. Because of abundant additional diffusion, B2-upwind simulations favorably suppress numerical wiggles, but pressure peaks are not properly predicted, the vortex street is too wide, and drag forces are usually over predicted. Close examination of the velocity field shows that pure 2nd-order central discretisation gives wiggles (well-known numerical artifact) in front of the cylinder and in the vortex region behind. The application of $C_2$ reduces wiggles, but small erroneous `wrinkles' are observed. This is currently under investigation; regular suppression of certain numerical modes in the turbulent signal seems to be of great help. The $C_2$ simulation gives a realistic wake prediction, see Fig. 10. More details can be found in Van der Heiden et al. 2012, Van der Plas et al. 2012.

In the future, the improved discretisation near solid walls will be investigated further. It will be combined with $C_2$ regularisation and the $C_2$ approach will be further refined. The near-wall modeling (influence of turbulent boundary layer) will be improved as well. Many practical coastal and offshore applications are highly turbulent, for which it is impossible to resolve the boundary layer with a sufficiently refined grid. In ComFLOW, the influence of the turbulent boundary layer will

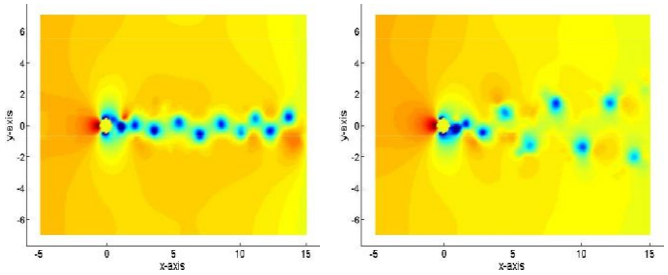


Fig. 10: Snapshots of the pressure field during vortex shedding behind a circular cylinder (Re=2000), with pure central discretisation (left) and central discretisation with $C_2$ regularisation (right).

be described with the model of Werner and Wengle 1991, where the effective wall shear stress is computed through a simple power-law approximation of the universal average velocity profile in the boundary layer. Obviously, the turbulence near the free-surface has to be described accurately as well for good predictions of hydrodynamic wave loading.

## COMPUTATIONAL EFFICIENCY

As a first step to increase the numerical efficiency, the pressure Poisson solver has been parallelised, since solving the pressure is the far most time-consuming part (up to 90% of the total time) of all the actions to be carried out each time step. Faster Poisson solvers are under consideration, e.g. Krylov methods with multi-grid pre-conditioning for acceleration, and parallelisation of other parts is foreseen. The numerical efficiency is also enhanced by extension of the applicability of the ABC, because of the possibility to reduce the computational domain. With regularisation turbulence models computing time is also saved (relatively), because of the lower need for grid resolution in comparison with LES/RANS models.

### Local Grid Refinement (LGR)

The numerical efficiency is further increased through local grid refinement (LGR). For accurate predictions of hydrodynamic forces, generally a high grid resolution is required near the structure. Further away, in less interesting parts of the flow domain, a coarser mesh is usually sufficient. Overall grid stretching leads to cells with unfavorable large aspect ratios. Therefore, in certain parts of the domain, cells are split into finer cells (see Fig. 11, left). The data structure in ComFLOW has been modified largely, by adding an additional index L to the indices (i,j,k) of a computational cell, indicating the refinement level. In this way, each cell of the coarse base grid (indicated by L=0) can be divided into finer cells (L=1), which can also be split-up (L=2), etc. The semi-structured method thus obtained allows for fast and efficient look-up, in comparison with the widely used tree-based methods. By making clever use of pointers, all existing subroutines can be used without modification. Only for the layers where the actual refinement takes place new subroutines are required, containing e.g. the discretisation of the momentum equations over the 1:2 refinement boundary.

For the discretisation near a grid refinement, special attention is required for the locations of variables. While setting up the discretised Poisson equation, coarse velocities are placed at the interface. The velocity u and pressure gradient $\delta p/\delta x$ are taken constant on the coarse cell face. Missing variables (see Fig. 11, right) are found from interpolation. As a result, a compact scheme is found for the pressure Poisson equation, with 1$^{st}$-order accuracy. In the literature, typically a

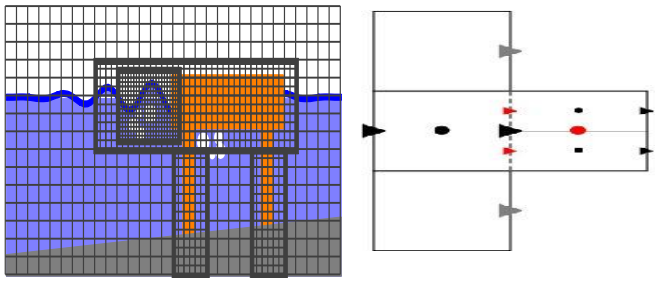

Fig. 11: LGR in the simulation of a wave around an offshore structure (left). Discretisation near the refinement involves known (black/grey) and virtual variables (red); cells are split with a 1:2 ratio (right).

larger stencil is used for the approximation (interpolation) of missing variables along the refinement interface. However, this increases the number of non-zero entries in the Poisson matrix, makes the matrix highly non-symmetric and probably destroys the diagonal dominance, which puts much higher demands on the linear solver. In the present approach, we seek to maintain symmetry of the discretization scheme in order to exploit the use of efficient and robust iterative solvers.

Simple test cases (e.g. Hagen-Poiseuille flow) indicate that the errors generated near refinement zones are generally very small; only little deviation from analytical solutions is found. The observed order during grid refinement equals the order found in cases without LGR. Hence, although the interface scheme is only 1$^{st}$-order accurate, the method provides an effective approach to saving computational time, while keeping the accuracy of the globally refined case. By restricting refinement interfaces to smooth areas of the flow, as is common practice, the convergence rate of the original scheme is effectively maintained. In Fig. 12, the flow around a circular cylinder is considered, with two levels of grid refinement near the cylinder. The snapshots of pressure and vorticity show that the flow goes through the refinement layers without visual disturbance. More details can be found in Van der Heiden et al. 2012, Van der Plas et al. 2012.

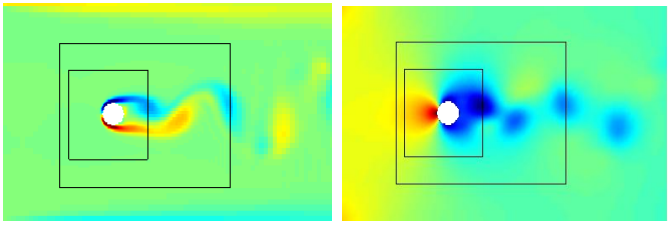

Fig. 12: Computed pressure distribution (left) and vorticity (right) for the flow around a circular cylinder (D=1m, $U_{in}$=1 m/s, Re = 100). The flow goes through the refinement layers without visual disturbance.

The advection of the free surface through refinement boundaries is currently investigated. The advection algorithm has been adjusted to the local changes in grid structure. Moreover, the LHF has been modified near the refinement, to get the correct $F_S$-sums in horizontal/vertical layers and hence the correct orientation of the free surface. First tests indicate that the disturbance is small when the free surface moves predominantly perpendicularly through the refinement. For other cases, the pressure boundary condition near the free-surface had to be adapted, to prevent instabilities near the free surface resulting from erroneous hydrostatic pressure effects.

## INTERACTIVE BODY MOTION (IBM)

In the offshore applications thus far studied with ComFLOW, the structure is kept fixed and the water flows against and/or around the structure. However, in many applications the object moves, often in full interaction with the fluid. For example, a ship at sea displaces water, and simultaneously the water waves exert hydrodynamic forces on the ship. In case of an LNG tanker, internal sloshing of LNG may affect the global motion (with risk of capsize) of the tanker and vice versa.

The first application of IBM with ComFLOW was the interaction between internal liquid sloshing and overall spacecraft dynamics. Experiments in space with the Sloshsat FLEVO satellite were supported by ComFLOW simulations (Veldman et al. 2007, Veldman 2006, Luppes et al. 2005, 2006, 2009b), see Fig. 13 (left). The Navier-Stokes equations for the fluid and the equations for solid-body dynamics were directly coupled and solved simultaneously. The influence of the moving fluid was accounted for by computing the variable centre of mass, moment of inertia and (pressure and viscous) forces on the tank wall every time step. ComFLOW was also used to study the interaction between water waves and the mechanical anchor constructions of a tension leg platform (TLP) (see Fig. 13, right), where the mechanical motion algorithm and the flow solver were also strongly intertwined (Johannessen et al. 2006).

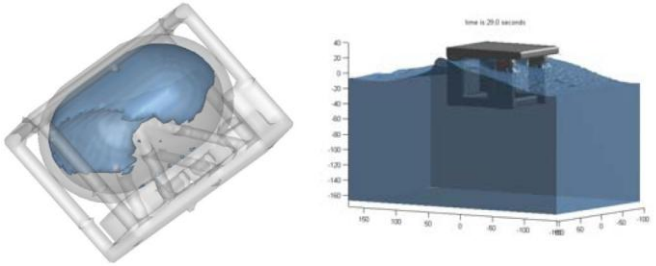

Fig. 13: Examples of IBM studies with ComFLOW: Sloshsat FLEVO (left) and Statoil Snorre TLP (right).

Unfortunately, direct coupling is not always possible, e.g. when ComFLOW is coupled to a commercial structural code (black box). However, a strong coupling is normally required for stability in case of large mass and/or inertia ratios. In the future, a quasi-simultaneous approach (Veldman 2009) will be applied. In this method, a simple approximation of the mechanical model is implemented as a preconditioner, to enhance convergence of the iterations between fluid and body. This usually provides sufficient stability of the coupling, also when the exact dynamical model is applied in the second step.

## CONCLUSIONS

The CFD simulation tool ComFLOW is developed for the accurate simulation of two-phase flow and wave impact in offshore and coastal applications. Over the years, several numerical techniques have been developed using ComFLOW. In this paper, a number of proven techniques have been presented: ABC to minimise numerical reflections from open boundaries, LHF for accurate free-surface displacement and gravity-consistent density averaging for two-phase flow to prevent spurious velocities near the free surface.

Several first steps and future plans to enlarge the functionality of ComFLOW have been discussed. The ABC has been extended for incoming and outgoing waves under an angle. The effect of viscosity in shear layers is more accurately described through regularisation turbulence modeling and improved discretisation of diffusion. With LGR the numerical efficiency has been increased. In the future the focus is on (propagation of) extreme waves and further improvement of both regularisation modeling and LGR. Also interactive vessel-wave dynamics will be subject of study.

## ACKNOWLEDGEMENTS

The research and development of ComFLOW are supported by the Dutch Technology Foundation STW, applied science division of NWO and the technology program of the Ministry of Economic Affairs in The Netherlands.

## REFERENCES

Botta, E.F.F., and Ellenbroek, M.H.M. (1985). "A modified SOR method for the Poisson equation in unsteady free-surface flow calculations", *J. Comp. Phys.*, 60:119–134.

Bunnik, T., Veldman, A.E.P., and Huijsmans, R.H.M (2007). "LNG sloshing simulations and validation model tests", *Proc. Int. Offshore and Polar Eng. Conf.*, ISOPE-2007.

Bunnik, T., Wellens, P., and Veldman, A. (2008). "Prediction of extreme wave loads in focused wave groups", *Proc. Int. Offshore and Polar Eng. Conf.*, ISOPE-2008, paper TPC-175.

Cheny, Y., and Botella, O. (2010). "The LS-STAG method: A new immersed boundary/level-set method for the computation of incompressible viscous flows in complex moving geometries with good conservation properties", *J. Comp. Phys.*, 229:1043–1076.

Düz, B., Huijsmans, R.H.M., Veldman, A.E.P., Borsboom, M.J.A., and Wellens, P.R. (2011a). "An absorbing boundary condition for regular and irregular wave simulations", *Proc. Int. Conf.*, MARINE 2011.

Düz, B., Huijsmans, R.H.M., Wellens, P.R., Borsboom, M.J.A., and Veldman, A.E.P. (2011b). "Towards a general-purpose open boundary condition for wave simulations", *Proc. 30th Int. Conf. on Ocean, Offshore and Arctic Eng.*, paper OMAE2011-49979.

Düz, B., Huijsmans, R.H.M., Wellens, P.R., Borsboom, M.J.A. and Veldman, A.E.P. (2012). "Application of an absorbing boundary condition in a wave-structure interaction problem", *Proc. 31st Int. Conf. on Ocean, Offshore and Arctic Eng.*, paper OMAE2012-83744.

Düz, B., Huijsmans, R.H.M., Veldman, A.E.P., Borsboom, M.J.A., and Wellens, P.R. (2013). "The effect of different Volume-Of-Fluid (VOF) methods on energy dissipation in simulations of propagating waves.", *Proc. Int. Conf.*, MARINE 2013.

Hirt, C.R., and Nichols, B.D. (1981). "Volume Of Fluid (VOF) Method for the Dynamics of Free Boundaries", *J. Comp. Phys.*, 39:201–225.

Johannessen, T.B., Haver, S., Bunnik, T., and Buchner, B. (2006). "Extreme wave effects on deep water TLP's", *Proc. Deep Offshore Techn. 2006*.

Kleefsman, K.M.T., Fekken, G., Veldman, A.E.P. and Iwanowski, B. (2004). "An improved Volume-Of-Fluid method for wave impact type problems", *Proc. 14th Int. Offshore and Polar Eng. Conf.*, ISOPE2004, Vol. I, pp. 334-341.

Kleefsman, K.M.T., Fekken, G., Veldman, A.E.P., Iwanowski, B., and Buchner, B. (2005a). "A Volume Of Fluid Based Simulation Method for Wave Impact Problems", *J. Comp. Phys.*, 206(1):363–393.

Kleefsman, K.M.T. (2005b). "Water impact loading on offshore structures - a numerical study", *PhD thesis University of Groningen*, The Netherlands.

Luppes, R., Helder, J.A., and Veldman, A.E.P. (2005). "Liquid sloshing in microgravity", *Proc. 56th Int. Astr. Congr.*, paper IAF-05-A2.2.07.

Luppes, R., Helder, J.A., and Veldman, A.E.P. (2006). "The numerical simulation of liquid sloshing in microgravity", Proc. *Eur. Conf.*

ECCOMAS CFD, ISBN 909020970-0, paper490.

Luppes, R., Wemmenhove, R., Veldman, A.E.P., and Bunnik, T. (2008). "Compressible Two-Phase Flow in Sloshing Tanks", Proc. *5th Eur. Conf.* ECCOMAS.

Luppes, R., Wellens, P.R., Veldman, A.E.P., and Bunnik, T. (2009a). "CFD simulations of wave run-up against a semi-submersible with absorbing boundary conditions", *Proc. Int. Conf.*, MARINE 2009.

Luppes, R., Helder, J.A., and Veldman, A.E.P. (2009b). "The numerical simulation of liquid sloshing in microgravity", *Proc. Comp. Fluid Dynamics 2006*, pages 607–612. ICCFD, doi: 10.1007/978-3-540-92779-2-95.

Luppes, R., Veldman, A.E.P., and Wellens, P.R. (2010a). "Absorbing Boundary Conditions for Wave Simulations around Offshore Structures", *Proc. Eur. Conf.*, ECCOMAS CFD.

Luppes, R., Veldman, A.E.P., and Wemmenhove, R. (2010b). "Simulation of two-phase flow in sloshing tanks", *Proc. Comp. Fluid Dynamics 2010*, pages 555–561. ICCFD, ISBN: 9783642178832.

Luppes, R., Düz, B., Van der Heiden, H.J.L., Van der Plas, P., and Veldman, A.E.P. (2011). "Numerical simulation of extreme wave impact on offshore platforms and coastal constructions". *Proc. V Int. Conf.*, MARINE 2011.

Van der Heiden, H.J.L., Van der Plas, P.., Veldman, A.E.P., Luppes, R., and Verstappen, R.W.C.P. (2012). "Efficiently Modeling Viscous Flow Effects by means of Regularization Turbulence Modeling and Local Grid Refinement", *Proc. Comp. Fluid Dynamics 2012*. ICCFD, paper ICCFD7-2504.

Van der Plas, P., Van der Heiden, H.J.L., Veldman, A.E.P., Luppes, R., and Verstappen, R.W.C.P. (2012). "Efficiently simulating viscous flow effects by means of regularization turbulence modeling and local grid refinement", *Proc. Eur. Conf.* ECCOMAS CFD, ISBN:978-3-9502481-9-7, paper 1474.

Veldman, A.E.P. (2006). "The simulation of violent free-surface dynamics at sea and in space". *Proc. Eur. Conf.* ECCOMAS CFD, ISBN 909020970-0, paper 492.

Veldman, A.E.P., Gerrits, J., Luppes, R., Helder, J.A., and Vreeburg, J.P.B. (2007). "The numerical simulation of liquid sloshing on board spacecraft", *J. Comp. Phys.*, 224:82–99.

Veldman, A.E.P. (2009). "A simple interaction law for viscous-inviscid interaction", *J. Eng. Math.*, 65:367–383.

Veldman, A.E.P., Luppes, R., Bunnik, T., Huijsmans, R.H.M., Düz, B., Iwanowski, B., Wemmenhove, R., Borsboom, M.J.A., Wellens, P.R., Van der Heiden, H.J.L., and Van der Plas, P. (2011). "Extreme wave impact on offshore platforms and coastal constructions", *Proc. 30th Int. Conf.*, OMAE2011-49488.

Verstappen, R.W.C.P., and Veldman, A.E.P. (2003). "Symmetry-Preserving Discretisation of Turbulent Flow", *J. Comp. Phys.*, 187:343–368.

Verstappen, R.W.C.P. (2008): "On restraining the production of small scales of motion in a turbulent channel flow", *Comp. Fluids*, 37:887–897.

Verstappen, R.W.C.P. (2011). "When does eddy viscosity damp sub-filter scales sufficiently?", *J. Sci. Comp*., 49(1):94-110.

Wellens, P.R., Luppes, R., Veldman, A.E.P., and Borsboom, M.J.A. (2009). "CFD simulations of a semisubmersible with absorbing boundary conditions", *Proc. 28th Int. Conf.* OMAE2009-79342.

Wemmenhove, R., Loots, G.E., and Veldman, A.E.P. (2006). "Numerical simulation of hydrodynamic wave loading by a two-phase model", *Proc. Eur. Conf.* ECCOMAS CFD, ISBN 909020970-0, paper 517.

Wemmenhove, R., Luppes, R., Veldman, A.E.P., and Bunnik, T. (2007). "Numerical simulation and model experiments of sloshing in LNG tanks", *Proc. Int. Conf.*, MARINE 2007.

Wemmenhove, R., Luppes, R., Veldman, A.E.P., and Bunnik, T. (2008a). "Application of a VOF Method to Model Compressible Two-Phase Flow in Sloshing Tanks", *Proc. 27th Int. Conf.*, OMAE2008-57254.

Wemmenhove, R. (2008b). "Numerical simulation of two-phase flow in offshore environments", *PhD thesis University of Groningen*, The Netherlands.

Wemmenhove, R., Iwanowski, B., Lefranc, M., Veldman, A.E.P., Luppes, R. and Bunnik, T. (2009). "Simulation of sloshing dynamics in a tank by an improved VOF method", *Proc. ISOPE 1st Sloshing Dynamics and Design Symposium*, paper ISOPE2009-YHK-05.

Wemmenhove, R., Luppes, R., Veldman, A.E.P. and Bunnik, T. (2012). "Simulation of hydrodynamic wave loading by a compressible two-phase flow method", *Proc. Violent Flows 2012*, ISBN 978-2-7483-9035-3, pp. 289-296.

Werner, H. and Wengle, H. (1991). "Large-eddy simulation of turbulent flow over and around a cube in a plate channel", *Proc. 8th Symp. on turbulent shear flows*, pages 155-168.

Youngs, D.L. (1982). "Time-dependent multi-material flow with large fluid distortion", In K.W. Morton and M.J. Baine, editors, *Numerical Methods for Fluid Dynamics*, pages 273–285. Academic Press, N.Y..